Drastic Decrease of the Curie Temperature in the Solid Solution $GdRu_xCd_{1-x}$

Frank Tappe, Falko M. Schappacher, Wilfried Hermes, Matthias Eul, and Rainer Pöttgen

Institut für Anorganische und Analytische Chemie and NRW Graduate School of Chemistry, Universität Münster, Corrensstraße 30, D-48149 Münster, Germany

Reprint requests to R. Pöttgen.
E-mail: pottgen@uni-muenster.de

Z. Naturforsch. **2009**, *64b,* 356 – 360;
received December 2, 2008

Five samples of solid solutions $GdRu_xCd_{1-x}$ extending up to $x \approx 0.25$ were synthesized by induction-melting of the elements in sealed tantalum tubes. According to X-ray powder diffraction data, the $GdRu_xCd_{1-x}$ samples crystallize with the cubic CsCl structure. The structures of two crystals were refined from diffractometer data: $Pm\bar{3}m$, a = 372.41(4) pm, $wR2$ = 0.0363, 45 F^2, 5 variables for $GdRu_{0.10(1)}Cd_{0.90(1)}$ and a = 367.70(4) pm, $wR2$ = 0.0301, 39 F^2, 5 variables for $GdRu_{0.20(1)}Cd_{0.80(1)}$. The cadmium-ruthenium substitution has a drastic effect on the magnetic properties. All samples order ferromagnetically, however, the Curie temperature decreases drastically from 258 K for GdCd to 63.6 K for $GdRu_{0.20}Cd_{0.80}$ with a Vegard-type behavior.

Key words: Intermetallics, Cadmium, Crystal Chemistry, Magnetic Properties

Introduction

In recent years we synthesized a family of RE_4TMg and RE_4TCd compounds (RE = rare earth element; T = late transition metal) [1, 2, and refs. therein] with the cubic Gd_4RhIn-type structure [3]. These rare earth metal-rich compounds have three crystallographically independent rare earth sites, and the structures contain the rare motif of Mg_4 and Cd_4 tetrahedra. Besides their crystal chemical peculiarities, we were also interested in the physical and chemical properties of these materials. An interesting example is Gd_4NiMg [4] which orders antiferromagnetically at T_N = 92 K. Gd_4NiMg absorbs up to 11 hydrogen atoms per formula unit and the resulting hydride Gd_4NiMgH_{11} remains paramagnetic down to 1.8 K.

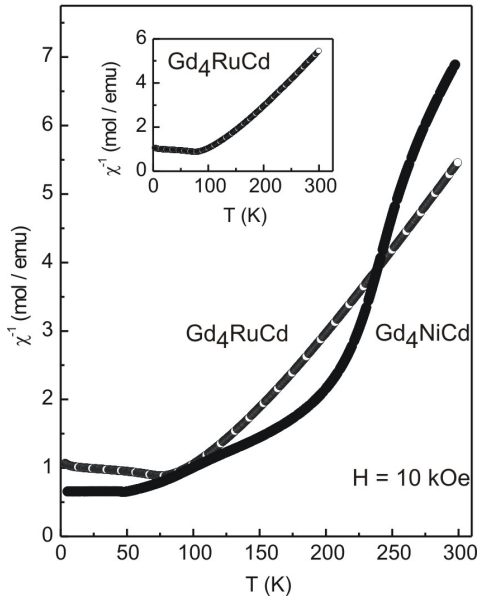

Fig. 1. Temperature dependence of the reciprocal magnetic susceptibility of Gd_4NiCd and Gd_4RuCd measured at an external field of 10 kOe.

When investigating the series of Gd_4TCd compounds, the susceptibility curves always revealed ferromagnetic impurities (strong negative curvatures in the χ^{-1} *vs.* T plots) which prevented a precise evaluation of the magnetic data. As an example we present the χ^{-1} *vs.* T plots for Gd_4NiCd and Gd_4RuCd in Fig. 1. More detailed investigations of these samples by X-ray powder diffraction and scanning electron microscopy in combination with EDX revealed the existence of impurity phases with a CsCl-related structure. We have then exemplarily studied the solid solution $GdRu_xCd_{1-x}$ where the cadmium site of GdCd [5] is substituted by ruthenium. Herein we report on the drastic influence of the Cd *vs.* Ru substitution on the magnetic properties, *i. e.* a breakdown of the Curie temperature from 258 K for GdCd [6] to 63.6 K for $GdRu_{0.20}Cd_{0.80}$.

Experimental Section

Synthesis

Starting materials for the preparation of the $GdRu_xCd_{1-x}$ samples were gadolinium turnings (Kelpin), ruthenium powder (Merck), and a cadmium rod (ChemPur), all with stated purities better than 99.9 %. The gadolinium turnings, ruthe-

Table 1. Lattice parameters of samples of the solid solutions $GdRu_xCd_{1-x}$.

Compound	a (pm)	V (nm^3)	Reference
GdCd	375.5(3)	0.0529	[5]
$GdRu_{0.05}Cd_{0.95}$	373.6(2)	0.0521	this work
$GdRu_{0.10}Cd_{0.90}$	371.7(2)	0.0514	this work
$GdRu_{0.10}Cd_{0.90}$[a]	372.41(4)	0.0517	this work
$GdRu_{0.15}Cd_{0.85}$	369.7(2)	0.0505	this work
$GdRu_{0.20}Cd_{0.80}$	367.8(2)	0.0498	this work
$GdRu_{0.20}Cd_{0.80}$[a]	367.70(4)	0.0497	this work
$GdRu_{0.25}Cd_{0.75}$	367.3(2)	0.0500	this work

[a] Single crystal data.

nium powder and pieces of the cadmium rod were weighed in the respective atomic ratios and arc-welded [7] in tantalum ampoules under an argon pressure of *ca*. 800 mbar. The argon was purified before with molecular sieves, silica gel, and titanium sponge (900 K). Subsequently the ampoules were placed in a water-cooled sample chamber [8] of an induction furnace (Hüttinger Elektronik, Freiburg, Typ TIG 1.5/300) and rapidly heated to *ca*. 1370 K. The samples were kept at that temperature for 5 min, then cooled to *ca*. 870 K within 5 min and kept at that temperature for another three hours. Finally the samples were quenched to r. t. by switching off the power supply of the high-frequency generator. The temperature was controlled through a Sensor Therm Methis MS09 pyrometer with an accuracy of ±30 K. The samples were mechanically broken off the tantalum ampoules. No reaction with the container material was observed. The samples are stable in air over several weeks.

For crystal growth of $GdRu_{0.1}Cd_{0.9}$ and $GdRu_{0.2}Cd_{0.8}$ the sealed tantalum tube was sealed in a quartz ampoule for oxidation protection, rapidly heated to 1470 K in a muffle furnace, kept at that temperature for 8 h, followed by slow cooling to 870 K at a rate of 3 K h^{-1}. Finally the sample was annealed for another 4 d at that temperature and then quenched to r. t. Single crystals exhibit metallic lustre while ground powder is dark grey.

EDX data

Semiquantitative EDX analyses of the two crystals investigated on the diffractometer were carried out with a Leica 420i scanning electron microscope with GdF_3, Ru, and Cd as standards. The experimentally observed compositions were close to the starting compositions of the samples. No impurity elements heavier than sodium (detection limit of the instrument) were found.

X-Ray diffraction

The polycrystalline $GdRu_xCd_{1-x}$ samples were characterized by Guinier patterns (imaging plate detector, Fujifilm BAS-1800) with Cu$K_{\alpha1}$ radiation and α-quartz (a = 491.30, c = 540.46 pm) as an internal standard. The cubic lattice parameters (Table 1) were deduced from least-squares refinements.

Table 2. Crystal data and structure refinement for $GdRu_{0.10(1)}Cd_{0.90(1)}$ and $GdRu_{0.20(1)}Cd_{0.80(1)}$.

Empirical formula	$GdRu_{0.10(1)}Cd_{0.90(1)}$	$GdRu_{0.20(1)}Cd_{0.80(1)}$
Unit cell dimensions	Table 1	Table 1
Molar mass, g mol^{-1}	268.52	267.38
Calcul. density, g cm^{-3}	8.63	8.93
Crystal size, μm^3	5 × 10 × 10	10 × 10 × 20
Transm. ratio (max/min)	0.590 / 0.358	0.333 / 0.137
Absorption coeff., mm^{-1}	41.3	42.6
Detector distance, mm	40	60
Exposure time, min	4	12
ω range; increment, deg	0 – 180; 1.0	0 – 180; 1.0
Integr. param. A; B; EMS	14.0; 2.5; 0.022	14.0; 4; 0.012
F(000), e	112	111
θ range, deg	5 – 38	5 – 35
Range in hkl	±6; ±6; ±6	±5; ±5; ±5
Total no. reflections	688	741
Independent refls. / R_{int}	45 / 0.0584	39 / 0.0580
Refls. with $I \geq 2\sigma(I)$	40	28
R_σ	0.0279	0.0246
Data / parameters	45 / 5	39 / 5
Goodness-of-fit on F^2	1.229	1.152
$R1$ / $wR2$ for $I \geq 2\sigma(I)$	0.0297 / 0.0362	0.0158 / 0.0290
$R1$ / $wR2$ for all data	0.0311 / 0.0363	0.0336 / 0.0301
Extinction coefficient	0.040(10)	0.085(12)
Largest diff. peak hole, e Å^{-3}	1.99 / −1.45	0.95 / −0.98

Small irregularly shaped single crystals of $GdRu_{0.1}Cd_{0.9}$ and $GdRu_{0.2}Cd_{0.8}$ were selected from the crushed samples. They were tested by Laue photographs on a Buerger camera using white Mo radiation. Intensity data were collected on a Stoe IPDS II diffractometer (graphite-monochromatized MoK_α radiation; oscillation mode). Numerical absorption corrections were applied to the data sets. All relevant details concerning the data collections and evaluations are listed in Table 2.

Structure refinement

Both data sets clearly showed primitive reflections in agreement with the CsCl-type structure. The gadolinium atoms were placed on the 1a site, and on the 1b site we allowed Ru/Cd mixing. The structures were then refined using SHELXL-97 [9] (full-matrix least-squares on F^2) with anisotropic atomic displacement parameters for all atoms. The final difference Fourier syntheses were flat (Table 2). The crystallographic data are listed in Table 3.

Further details of the crystal structure investigations may be obtained from Fachinformationszentrum Karlsruhe, 76344 Eggenstein-Leopoldshafen, Germany (fax: +49-7247-808-666; e-mail: crysdata@fiz-karlsruhe.de, http://www.fiz-informationsdienste.de/en/DB/icsd/depot_anforderung.html) on quoting the deposition numbers CSD-420131 ($GdRu_{0.10}Cd_{0.90}$) and CSD-420132 ($GdRu_{0.20}Cd_{0.80}$).

Table 3. Atomic coordinates and isotropic displacement parameters (pm^2) for $GdRu_{0.10(1)}Cd_{0.90(1)}$ and $GdRu_{0.20(1)}Cd_{0.80(1)}$. ($U_{eq}$ is defined as one third of the trace of the orthogonalized U_{ij} tensor).

Atom	Wyckoff position	Occupancy (%)	x	y	z	U_{iso} / U_{eq}
$GdRu_{0.10(1)}Cd_{0.90(1)}$:						
Gd	1*a*	100	0	0	0	170(5)
Ru	1*b*	10(1)	1/2	1/2	1/2	197(6)
Cd	1*b*	90(1)	1/2	1/2	1/2	197(6)
$GdRu_{0.20(1)}Cd_{0.80(1)}$:						
Gd	1*a*	100	0	0	0	289(6)
Ru	1*b*	20(1)	1/2	1/2	1/2	219(5)
Cd	1*b*	80(1)	1/2	1/2	1/2	219(5)

Physical property measurements

The $GdRu_xCd_{1-x}$ samples were packed in kapton foil and attached to the sample holder rod of a VSM for measuring the magnetic properties in a Quantum Design Physical-Property-Measurement-System in the temperature range 3.1 – 305 K with magnetic flux densities up to 80 kOe.

Discussion

Crystal chemistry

The binary CsCl-type compound GdCd [5] shows a solid solution $GdRu_xCd_{1-x}$ up to $x \approx 0.25$ (Fig. 2). Due to the smaller size of the ruthenium atoms, the cubic lattice parameter decreases with increasing ruthenium content with a Vegard-type behavior (Fig. 3). Already at $x \approx 0.25$ we observed small deviations from the Vegard behavior and the occurrence of secondary phases in the powder pattern. The boundary of the solid solution is thus between $x = 0.20$ and 0.25. For GdCd the Gd–Gd and Gd–Cd distances are 376 and 326 pm, respectively. They decrease to 368 and 319 pm for $x = 0.2$ (Table 1). The ruthenium/cadmium mixing induces drastic inhomogeneities in the first gadolinium coordination sphere, strongly influencing the magnetic coupling (*vide infra*).

Magnetic behavior

GdCd orders ferromagnetically at 258 K [6]. The same type of magnetic ordering is also observed within the solid solution $GdRu_xCd_{1-x}$, however, with distinctly lower Curie temperatures. As an example we present the magnetic data of $GdRu_{0.2}Cd_{0.8}$ in Fig. 4. Above 100 K we observed Curie-Weiss behavior (Fig. 4a) with an experimental magnetic moment of 8.11(1) μ_B formula unit^{-1} and a Weiss constant of 70.4(1) K indicating ferromagnetic interactions. The experimentally determined magnetic moment is slightly larger than the free ion value of 7.94 μ_B for Gd^{3+}. Slightly enhanced moments are frequently observed for gadolinium intermetallics and can be ascribed to $4f$-$5d$ exchange interactions, with a contribution from d electrons originating mainly from the gadolinium ions. The precise Curie temperature of 63.6(1) K was determined from a zero-field-cooling field-cooling measurement at low external field strength (Fig. 4b). The magnetization behavior (Fig. 4c) is typical for a soft ferromagnet. The saturation magnetization at 5 K and 80 kOe is 7 μ_B per gadolinium atom and perfectly matches the theoretical value ($g \times J = 7\ \mu_B$), indicating full parallel spin alignment. At 5 K we observe a minor hysteresis (Fig. 4d). The other members of the solid solutions show similar behavior. The derived data are summarized in Table 4.

The small degree of Ru/Cd mixing leads to a drastic decrease of the Curie temperature from 258 K (GdCd) to 63.6 K ($GdRu_{0.2}Cd_{0.8}$) in a Vegard-type manner

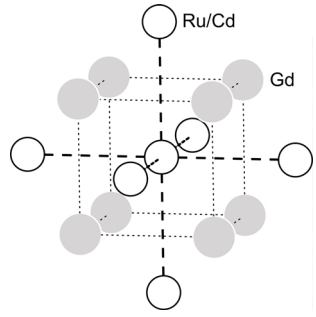

Fig. 2. The CsCl-type crystal structure of $GdRu_xCd_{1-x}$.

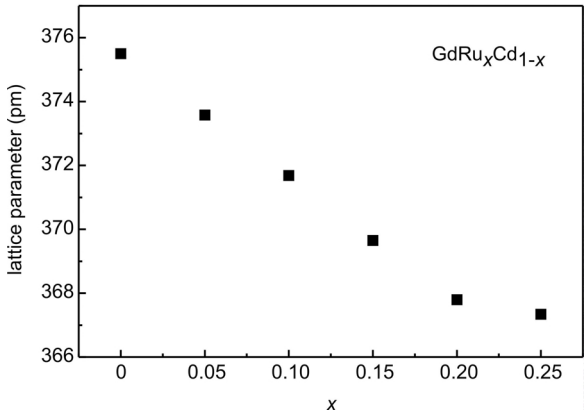

Fig. 3. Course of the lattice parameter in the CsCl-type solid solution $GdRu_xCd_{1-x}$.

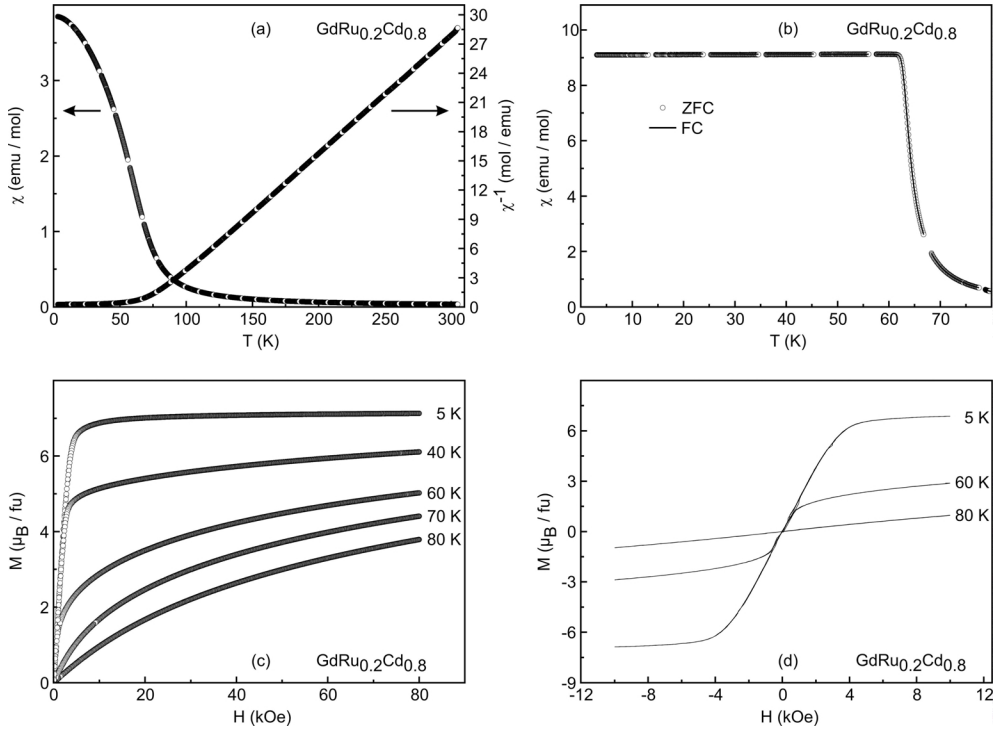

Fig. 4. Magnetic properties of $GdRu_{0.2}Cd_{0.8}$: a) χ and χ^{-1} *vs.* T measured at 10 kOe, b) zero-field-cooled and field-cooled susceptibility measured at 100 Oe, c) magnetization isotherms at various temperatures, d) hysteresis loops measured at T = 5, 60 and 80 K.

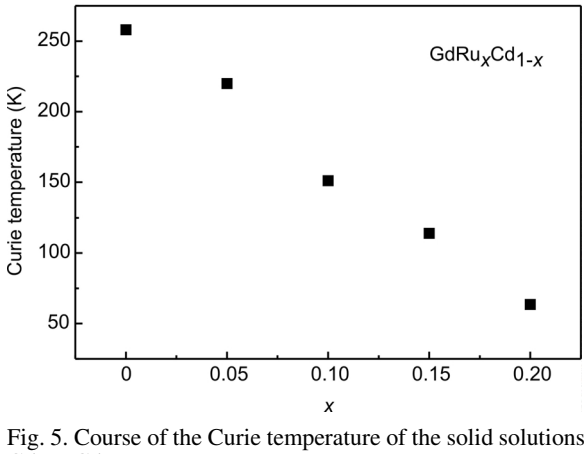

Fig. 5. Course of the Curie temperature of the solid solutions $GdRu_xCd_{1-x}$.

(Fig. 5). The disorder in the Ru/Cd substructure drastically disturbs the Gd–Gd coupling and leads to the strong decrease in the ordering temperature. Similar behavior is expected for related solid solutions, and also for the magnesium-based systems.

Table 4. Magnetic properties of samples of the solid solutions $GdRu_xCd_{1-x}$: T_C, Curie temperature; Θ_P, paramagnetic Curie temperature; μ_{eff}, effective magnetic moment in the paramagnetic range.

Compound	T_C (K)	Θ_P (K)	μ_{eff} (μ_B per Gd atom)	Reference
GdCd	258	–	–	[6]
$GdRu_{0.05}Cd_{0.95}$	220.3(5)	222.6(2)	7.81(1)	this work
$GdRu_{0.10}Cd_{0.90}$	151.0(5)	164.7(2)	7.73(1)	this work
$GdRu_{0.15}Cd_{0.85}$	114(1)	119.2(2)	7.89(1)	this work
$GdRu_{0.20}Cd_{0.80}$	63.6(1)	70.4(1)	8.11(1)	this work

Acknowledgements

This work was financially supported by the Deutsche Forschungsgemeinschaft within SPP 1166. W. H. is indebted to the Fonds der Chemischen Industrie for a Ph. D. fellowship.

[1] F. M. Schappacher, U. Ch. Rodewald, R. Pöttgen, *Z. Naturforsch.* **2008**, *63b*, 1127.
[2] S. Tuncel, B. Chevalier, R. Pöttgen, *Z. Naturforsch.* **2008**, *63b*, 600.
[3] R. Zaremba, U. Ch. Rodewald, R.-D. Hoffmann, R. Pöttgen, *Monatsh. Chem.* **2007**, *138*, 523.
[4] S. Tuncel, J. G. Roquefère, C. Stan, J.-L. Bobet, B. Chevalier, E. Gaudin, R.-D. Hoffmann, U. Ch. Rodewald, R. Pöttgen, *J. Solid State Chem.* **2009**, *182*, 229.
[5] C. C. Chao, P. Duwez, *J. Appl. Phys.* **1966**, *37*, 2631.
[6] R. Aléonard, P. Morin, *J. Magn. Magn. Mater.* **1985**, *50*, 128.
[7] R. Pöttgen, Th. Gulden, A. Simon, *GIT Labor-Fachzeitschrift* **1999**, *43*, 133.
[8] D. Kußmann, R.-D. Hoffmann, R. Pöttgen, *Z. Anorg. Allg. Chem.* **1998**, *624*, 1727.
[9] G. M. Sheldrick, SHELXL-97, Program for Crystal Structure Refinement, University of Göttingen, Göttingen (Germany) **1997**.